European Journal of Pharmacology 782 (2016) 59–69

Contents lists available at ScienceDirect

European Journal of Pharmacology

journal homepage: www.elsevier.com/locate/ejphar

Immunopharmacology and inflammation

Gene expression profiling reveals novel protective effects of Aminaphtone on ECV304 endothelial cells

Giulia Salazar [a,*], Chiara Bellocchi [a], Katia Todoerti [b], Federica Saporiti [c], Luca Piacentini [c], Raffaella Scorza [a], Gualtiero I. Colombo [c]

[a] Referral Centre for Systemic Autoimmune Diseases, University of Milan and Fondazione IRCCS Ca' Granda Ospedale Maggiore Policlinico, Milano, Italy
[b] Laboratory of Preclinical and Translational Research, IRCCS-CROB, Referral Cancer Centre of Basilicata, Rionero in Vulture, Italy
[c] Laboratory of Immunology and Functional Genomics, Centro Cardiologico Monzino IRCCS, Milan, Italy

ARTICLE INFO

Article history:
Received 4 June 2015
Received in revised form
7 April 2016
Accepted 11 April 2016
Available online 12 April 2016

Keywords:
Endothelial cells
Endothelin-1
Gene expression profiling
Cytokines
Inflammation

Chemical compounds studied in this article:
Aminaphtone (PubChem CID: 84621)

ABSTRACT

Aminaphtone, a drug used in the treatment of chronic venous insufficiency (CVI), showed a remarkable role in the modulation of several vasoactive factors, like endothelin-1 and adhesion molecules. We analysed *in vitro* the effects of Aminaphtone on whole-genome gene expression and production of different inflammatory proteins. ECV-304 endothelial cells were stimulated with IL-1β 100 U/ml in the presence or absence of Aminaphtone 6 μg/ml. Gene expression profiles were compared at 1, 3, and 6 h after stimulation by microarray. Supernatants of ECV-304 cultures were analysed at 3, 6, 12, and 24 h by multiplex ELISA for production of several cytokine and chemokines. Microarrays showed a significant down-regulation at all times of a wide range of inflammatory genes. Aminaphtone appeared also able to modulate the regulation of immune response process (down-regulating cytokine biosynthesis, transcripts involved in lymphocyte differentiation and cell proliferation, and cytokine-cytokine receptor interaction) and to regulate genes engaged in homeostasis, secretion, body fluid levels, response to hypoxia, cell division, and cell-to-cell communication and signalling. Results were confirmed and extended analysing the secretome, which showed significant reduction of the release of 14 cytokines and chemokines. These effects are predicted to be mediated by interaction with different transcription factors.

Aminaphtone was able to modulate the expression of inflammatory molecules relevant to the pathogenesis of several conditions in which the endothelial dysfunction is the main player and early event, like scleroderma, lung fibrosis, or atherosclerosis.

1. Introduction

Aminaphtone (C18-H15-N-O4) is a synthetic molecule derived from 4-aminobenzoic acid, which is currently employed in the management of capillary disorders. The drug has been used both to treat and prevent late complications of patients affected by chronic venous insufficiency (CVI) of the lower limbs, efficiently reducing vessel permeability and the number and size of leg ulcers (Doni et al., 1983; Smith, 2001; Villaverde et al., 1989). It has been suggested that Aminaphtone increases capillary resistance by the inhibition of hyaluronidases, and a few published case reports showed that the drug is effective in reducing oedema in idiopathic cyclic oedema (Pereira de Godoy, 2008) and ameliorating purpuric lesions in Schamberg's disease (de Godoy and Batigalia, 2009). Despite this, little is known about the effects of Aminaphtone at molecular level.

Previous works from our group investigated whether Aminaphtone down-regulates molecules with key vasoactive roles. First, we examined whether Aminaphtone modulates the expression of the vasoconstrictive molecule endothelin-1 in endothelial cells (ECs). Endothelin-1 is involved in CVI pathogenesis, as prolonged venous stasis and hypoxia-induced vasoconstriction determine ischemia with consequent smooth muscle cell activation, decrement of nitric oxide (NO), and overexpression of endothelin-1, which in turn exacerbates ischemia. We demonstrated that Aminaphtone was able to decrease endothelin-1, both at mRNA and protein level, in ECV304 EC-line stimulated with IL-1β, in a

Nonstandard abbreviations: CVI, chronic venous insufficiency; ECs, endothelial cells; NO, nitric oxide; PAH, Pulmonary Arterial Hypertension; TFs, transcription factors

* Correspondence to: Laboratory of Immunology, Fondazione IRCCS Ca' Granda Ospedale Maggiore Policlinico, via Pace 9, 20121 Milano, Italy.
E-mail address: g.salazar@hotmail.it (G. Salazar).

http://dx.doi.org/10.1016/j.ejphar.2016.04.018

dose and time-dependent manner (Scorza et al., 2008a).

Given the involvement of endothelin-1 in the pathogenesis of Pulmonary Arterial Hypertension (PAH) (Giaid et al., 1993), we studied the action of Aminaphtone *in vivo* in a rat model of monocrotaline-induced PAH (Zambelli et al., 2011). Aminaphtone at the highest dose reduced plasma concentration of endothelin-1, attenuated right ventricular hypertrophy, and lessened the wall thickness of the pulmonary arteries, which are a direct morphological consequence of high levels of endothelin-1.

Furthermore, we analysed the influence of Aminaphtone on the regulation of adhesion molecules *in vivo*. In a 12-week prospective, randomized, open-label pilot study on 24 patients with Systemic Sclerosis, of whom 12 were controls and 12 were treated with Aminaphtone 75 mg *ter in die*, we observed a decrease in the concentrations of circulating soluble adhesion molecules. The effect of Aminaphtone appeared to be preferentially exerted on soluble endothelium leukocyte adhesion molecule 1 (sELAM-1) and vascular cell adhesion molecule 1 (sVCAM-1) (Scorza et al., 2008b).

In this work, we seek to explore the actions of Aminaphtone at the molecular level. In particular, we focused our attention on whether it favourably modulates inflammatory pathways. To this end, we used the microarray technology to investigate the global gene expression profile and its modulation over time in a human EC model subjected to an inflammatory stimulus and/or treatment with Aminaphtone. We then confirmed and extended our observation at post-transcriptional level, by quantifying different pro-inflammatory mediators in cell culture supernatants using multiplex bead-based and singleplex ELISA techniques.

2. Materials and methods

2.1. Cell culture and treatments

Human ECV304 endothelial cells (ECACC No. 92091712) were grown in M199 medium (Invitrogen, Carlsbad, CA) supplemented with 10% foetal bovine serum (FBS; Hyclone, Logan, UT), 50 U/ml penicillin, and 50 U/ml streptomycin in a 37 °C humidified incubator with 5% CO_2. Cells were seeded at 4×10^5/well in 6-well tissue-culture treated plates. Twenty-four h before treatment, cells were serum starved (1% FBS) in order to synchronize the mitotic phase.

Aminaphtone was generously gifted by Baldacci S. p. A., Pisa, Italy. The lyophilized drug was first diluted with dimethyl sulfoxide (Sigma-Aldrich, St. Louis, MO), and then 1:10 with Dulbecco's phosphate buffered saline without calcium and magnesium to a concentration of 0.1 mg/ml. This solution was further diluted with complete M199 to a 6 μg/ml final concentration, which roughly corresponds to the drug peak plasma concentration that can be observed in healthy subjects after an oral administration of Aminaphtone 75 mg (Scorza et al., 2008b).

Confluent ECV304 cells were incubated for 1, 3, 6, 12, and 24 h with recombinant interleukin-1β (IL-1β; Sigma-Aldrich) 100 IU/ml in the presence of Aminaphtone 6 μg/ml or an equal volume of medium alone. All experiments were performed in two separate series of three independent replicates for each time point. Gene expression analysis was performed at 1, 3, and 6 h-time points; protein detection in the supernatants was executed at 3, 6, 12, and 24 h.

2.2. RNA extraction

Total RNA extraction was performed using the TRIzol Reagent (Life Technologies, Rockville, MD) directly added to the EC culture plates after 1, 3, and 6-h treatment, following the manufacturer's protocol. Genomic DNA contamination was eliminated treating RNA samples with RNase-free Turbo DNase (Life Technologies) for 15 min at room temperature. RNA quantity and purity were evaluated using an Infinite 200 PRO plate reader (Tecan, Männedorf, Switzerland) for micro-volume spectrophotometry; quality and integrity were checked by the RNA 6000 Nano kit with a Bioanalyzer 2100 (Agilent Technologies, Santa Clara, CA). The ratio of absorbance at 260 and 280 nm was ≥ 1.9 and the RNA integrity number (RIN) was > 8 for all samples.

2.3. Whole-genome gene expression analysis

The RNA samples from the first experimental series of three independent replicates, collected at 1, 3, and 6 h after treatment, were used for gene expression profiling. Preparation of DNA single-stranded sense target, hybridization to GeneChip Gene 1.0 ST Arrays (Affymetrix, Santa Clara, CA), and scanning of the chips on an Affymetrix 7G Scanner were carried out according to manufacturer's protocols.

The RMAExpress software version 1.0.5 was used for background adjustment, quantile normalization, and probe set summarization by the Robust Multi-array Average (RMA) procedure (Bolstad et al., 2003; Irizarry et al., 2003). Probe sets mapping on the same gene were considered as single series of expression value by means of the median polish summarization algorithm. Gene filtering and annotation were performed using BRB-ArrayTools version 4.3.2 developed by Dr. Richard Simon and BRB-ArrayTools Development Team and *R* packages available from Bioconductor release 2.12 (Gentleman et al., 2004). Probe sets with a mean intensity less than 10 in at least one time point in one of the treatment class (corresponding to a low but robust expression level) were filtered out. Genes showing minimal variation across the samples, *i.e.* with a *P*-value of the log-ratio variation greater than 0.01, were deemed as non-informative and excluded from further analysis. Multiple probe sets were reduced to one per gene symbol by using the most variable probe set measured by interquartile range across arrays. Project was annotated by Bioconductor annotation package hugene10sttranscriptcluster.db version 8.0.1.

Differentially expressed genes were identified combining two different approaches, using algorithms incorporated in the open-source software MultiExperiment Viewer (MeV) version 4.9 (Saeed et al., 2003). First we used the Bayesian Estimation of Temporal Regulation (BETR) method (Aryee et al., 2009), to identify genes that vary significantly between the two conditions across time points. BETR is a linear random-effect modelling framework that takes into account correlations within samples between sampling times. Genes assigned an *alpha* value less than 0.1, *i.e.* an acceptable False Discovery Rate (FDR) $< 10\%$, were deemed significantly different. Then, given the balanced factorial design of the study, we used a two-factor ANOVA to determine which genes were mainly influenced by the treatment effect *per se* (Aminaphtone) and/or by the interaction effect of the two factors (time and treatment). Genes were considered statistically significant if the *P*-values (for treatment and/or interaction), computed from the F-distribution, were less than 0.05. This was followed by pairwise comparisons to identify significantly different gene expression at *alpha* less than 0.05 (Student's 2-tailed *t*-test) between treatment classes at any time points.

Hierarchical cluster analysis was performed to visualize the similarity and differences in gene expression profiles among the samples, using the algorithm implemented in BRB-ArrayTools. Log_2 transformed normalized gene expression values were median-centred and scaled and clustered by Pearson's centred correlation and average linkage.

We then used a clustering algorithm called CLICK (CLuster Identification via Connectivity Kernels), implemented in the java-based tool EXPression ANalyzer and DisplayER (EXPANDER) v6.3

(Sharan et al., 2003), to identify clusters of co-regulated genes with distinct temporal patterns between the two conditions. CLICK makes use of graph-theoretic and statistical techniques to recognize tight groups of highly similar elements. We used the algorithm with the default homogeneity parameter $=0.65$ for a balanced intra-cluster similarity and inter-cluster separation.

Functional analysis on the entire dataset of significant genes identified by BETR was performed by examining gene sets for differential expression among the treatment classes. The gene sets were defined based on Gene Ontology (GO) terms (http://www.geneontology.org) (The Gene Ontology Consortium, 2015), the Kyoto Encyclopaedia of Genes and Genomes (KEGG) pathway database (http://www.genome.jp/kegg/pathway.html), and the Broad Institute Molecular Signature Database (MsigDB; curated gene sets) (Subramanian et al., 2005). To find significant gene sets we used the LS/KS permutation tests, which find gene sets with more genes differentially expressed among the phenotype classes than expected by chance. The threshold for determining significant gene sets was *P*-value lower than 0.005. Redundant GO terms were removed using the web-based tool REViGO (Supek et al., 2011), with an allowed similarity threshold of 0.5. Not pertinent gene sets were manually removed.

Functional analysis of the gene clusters identified by CLICK was carried out using the TANGO (Tool for ANalysis of GO enrichments) algorithm implemented in EXPANDER, which performs hypergeometric enrichment tests on GO terms and corrects for multiple testing by bootstrapping (1000 bootstraps), thus estimating the empirical *P*-value distribution for the evaluated sets. A functional class was considered significantly enriched in a cluster of co-regulated genes (as detected above) if its corrected *P*-value was lower than 0.05. Similarly, we conducted a KEGG pathway enrichment analysis by hyper-geometric enrichment tests, correcting for multiple testing using the Bonferroni correction.

Finally, using the PRIMA (PRomoter Integration in Microarray Analysis) algorithm, we identified transcription factors (TFs) whose binding sites are significantly over-represented in the promoters of genes within each cluster pointed out by CLICK. A TF binding site was considered significantly enriched in a cluster if its *P*-value was lower than 5×10^{-4}. The gene sets were defined based on experimentally determined TF binding sites derived from the TRANSFAC Database (http://www.gene-regulation.com) (Wingender, 2008).

2.4. Reverse transcription quantitative-PCR validation

The same RNA samples used for microarray profiling, together with a second series of three independent replicates, were used for PCR validation. First-strand complementary DNA (cDNA) for single target gene expression analysis was synthesized from 3 μg of total RNA for each sample using the High Capacity cDNA Reverse Transcription Kit (Life Technologies). Expression of *CSF3*, *IGFL1*, *TGFB2*, *TNF*, *TNFRSF11B*, *TNFSF18* (cf. Table 1 in Ref. Salazar et al., submitted for publication, for gene names), and the endogenous control genes β-actin (*ACTB*), glyceraldehyde-3-phosphate dehydrogenase (*GAPDH*), and hypoxanthine guanine phosphoribosyl transferase 1 (*HPRT1*) was measured by reverse transcription (RT) quantitative-PCR (RT-qPCR) using single TaqMan Gene Expression Assays run on the Vii7A real-time PCR System (Life Technologies). TaqMan Gene Expression Master Mix and cDNA sample (20 ng/well) were handled with a MICROLAB STAR robotic station (Hamilton Robotics, Bonaduz, Switzerland), to standardize liquid handling and minimize manual error. Three replicates of each gene for each sample were run in a 384-well format plate. The following TaqMan-based assays were used: Hs00357085_g1 (*CSF3*), Hs01651089 (*IGFL1*), Hs00234244_m1 (*TGFB2*), Hs00900358_m1 (*TNFRSF11B*), Hs00183225_m1 (*TNFSF18*), Hs01060665_g1 (*ACTB*), Hs02758991_g1 (*GAPDH*), and Hs99999909_m1 (*HPRT1*) (all from Life Technologies), and Hs. PT.56a.41006330 (TNF-α) (Integrated DNA Technologies, Coralville, IA). Experimental threshold and baseline were calculated by the algorithm of the Vii7A RUO Software v1.2 (Life Technologies), and data were analysed by the corrected ΔΔCt method (Pfaffl, 2001).

Table 1
Top 25 differentially expressed genes in Aminaphtone-treated *vs.* untreated IL-1β stimulated endothelial cells, according to BETR analysis.

					Fold-change			P_{pairw}		
Symbol	**Name**	**FDR**	P_{treatm}	$P_{interact}$	**1 h**	**3 h**	**6 h**	***1 h***	***3 h***	***6 h***
BNIP3	BCL2/adenovirus E1B 19 kDa interacting protein 3	$<1\times10^{-7}$	$<1\times10^{-4}$	$<1\times10^{-5}$	1.1	−1.1	−2.5			[b]
CCL22	chemokine (C-C motif) ligand 22	$<1\times10^{-7}$	$<1\times10^{-5}$	*ns*	−1.4	−2.2	−2.0	[a]	[b]	[b]
EBI3	Epstein-Barr virus induced 3	$<1\times10^{-7}$	$<1\times10^{-5}$	*ns*	−1.8	−1.7	−2.1	[b]	[b]	[b]
EDN1	endothelin 1	$<1\times10^{-7}$	$<1\times10^{-5}$	*ns*	−1.8	−1.9	−2.0	[b]	[b]	[b]
HIST2H4A	histone cluster 2, H4a	$<1\times10^{-7}$	$<1\times10^{-6}$	<0.05	1.9	1.5	1.3	[b]	[b]	[b]
IGFL1	IGF-like family member 1	$<1\times10^{-7}$	$<1\times10^{-4}$	*ns*	−2.1	−2.0	−2.4	[b]	[b]	[b]
MMP10	matrix metallopeptidase 10 (stromelysin 2)	$<1\times10^{-7}$	<0.001	<0.01	−1.0	−1.4	−2.4		[a]	[b]
MYLIP	myosin regulatory light chain interacting protein	$<1\times10^{-7}$	$<1\times10^{-6}$	$<1\times10^{-4}$	2.8	1.5	1.1	[b]	[b]	
PFKFB4	6-phosphofructo-2-kinase/fructose-2,6-biphosphatase 4	$<1\times10^{-7}$	<0.001	$<1\times10^{-4}$	−1.1	1.0	−2.7			[b]
PRDM1	PR domain containing 1, with ZNF domain	$<1\times10^{-7}$	$<1\times10^{-4}$	$<1\times10^{-5}$	−2.5	−1.0	−1.0	[b]		
S100A3	S100 calcium binding protein A3	$<1\times10^{-7}$	$<1\times10^{-5}$	*ns*	−2.4	−1.4	−2.0	[b]		[b]
TNFSF18	tumor necrosis factor (ligand) superfamily, member 18	$<1\times10^{-7}$	$<1\times10^{-5}$	*ns*	−2.4	−4.2	−3.4	[b]	[b]	[b]
CNNM4	cyclin M4	$<1\times10^{-6}$	$<1\times10^{-4}$	<0.001	−1.1	2.0	1.6		[b]	[b]
EVA1A	eva-1 homolog A (C. elegans)	$<1\times10^{-5}$	$<1\times10^{-6}$	<0.01	−1.2	−1.5	−1.7	[a]	[b]	[b]
HK2	hexokinase 2	$<1\times10^{-5}$	<0.001	<0.01	1.1	−1.4	−2.3		[a]	[b]
PDK1	pyruvate dehydrogenase kinase, isozyme 1	$<1\times10^{-5}$	<0.05	<0.001	1.4	−1.2	−2.4	[a]		[b]
FOS	FBJ murine osteosarcoma viral oncogene homolog	$<1\times10^{-5}$	<0.001	<0.001	2.1	1.0	1.1	[b]		
TNFRSF11B	tumor necrosis factor receptor superfamily, member 11b	$<1\times10^{-5}$	<0.001	*ns*	−1.5	−2.6	−1.7		[b]	[a]
PLCB4	phospholipase C, beta 4	$<1\times10^{-5}$	<0.05	<0.01	1.7	−2.1	−2.1	[a]	[b]	[b]
TGFB2	transforming growth factor, beta 2	$<1\times10^{-4}$	<0.01	<0.01	1.2	−2.1	−1.5		[b]	[a]
MMP3	matrix metallopeptidase 3 (stromelysin 1, progelatinase)	$<1\times10^{-4}$	<0.01	<0.05	−1.0	−1.6	−2.6		[a]	[b]
CYP24A1	cytochrome P450, family 24, subfamily A, polypeptide 1	$<1\times10^{-4}$	$<1\times10^{-4}$	*ns*	−1.5	−1.7	−1.5	[b]	[b]	[b]
DKK1	dickkopf 1 homolog (Xenopus laevis)	$<1\times10^{-4}$	$<1\times10^{-4}$	<0.05	−1.2	−1.2	−1.9			[b]
ELMSAN1	ELM2 and Myb/SANT-like domain containing 1	$<1\times10^{-4}$	<0.05	$<1\times10^{-4}$	−1.9	1.2	1.1	[b]	[a]	
KCTD11	potassium channel tetramerisation domain containing 11	$<1\times10^{-4}$	<0.001	*ns*	−1.9	−1.4	−1.7	[b]		[b]

FDR: *P*-values corrected for the false discovery rate, at the BETR analysis. P_{treatm}: *P*-values for the treatment effect; and $P_{interact}$: *P*-values for the interaction effect between time and treatment, at two-factor ANOVA. P_{pairw}: significance level for post-hoc pairwise comparisons: [a] $P<0.05$; [b] $P<0.01$.

Raw expression intensities of target mRNAs were normalized to the mean intensity of the three most stable endogenous control genes (*ACTB*, *GAPDH*, and *HPRT1*) selected from a set of eight (the aforementioned plus β-2-microglobulin, phosphoglycerate kinase 1, pumilio homolog 1, ribosomal protein large P0, secretogranin V, and tyrosine 3-monooxygenase/tryptophan 5-monooxygenase activation protein zeta polypeptide). Analysis of gene expression stability and selection of the best reference genes were performed using the NormFinder version 0.953 Excel Add-In (Andersen et al., 2004) on the RMA expression values.

2.5. Cytokine measurement in the secretome

Supernatants were collected at 3, 6, 12, and 24 h after treatment with IL-1β with or without Aminaphtone. All samples were from the same two series used for gene expression analysis, which included three independent experiments each. The concentrations of 30 cytokines/chemokines were measured by bead based multiplexing technique, using the Human Cytokine Magnetic 30-plex Panel Assay (Life Technologies) according to the manufacturer's protocol. Namely, the cytokines tested were: IL-1β, IL-1 receptor α (IL-1RA), IL-2, IL-2 receptor (IL-2R), IL-4, IL-5, IL-6, IL-7, IL-8, IL-10, IL-13, IL-15, IL-17, basic fibroblast growth factor (FGF-basic), epidermal growth factor (EGF), EOTAXIN, hepatocyte growth factor (HGF), granulocyte colony-stimulating factor (G-CSF), granulocyte-macrophage colony-stimulating factor (GM-CSF), interferon-alpha (IFN-α), interferon-gamma (IFN-γ), interferon gamma-induced protein 10 (IP-10) macrophage inflammatory protein-1-alpha (MIP-1α), macrophage inflammatory protein-1-beta (MIP-1β), macrophage migration inhibitory factor (MIF), monocyte chemotactic protein-1 (MCP-1), monokine induced by gamma interferon (MIG), RANTES, tumor necrosis factor-alpha (TNF-α), vascular endothelial growth factor (VEGF). Analyte readings were taken in a Bio-Plex 2200 reader and calculated using the software Bio-Plex Manager version 6.0 (Bio-Rad Laboratories, Hercules, CA). Assay sensitivity was >5 pg/ml for each analyte. Signal quantification was based on standard bead curves run in parallel to the test, using nonlinear 5-parameter logistic equations when fitting data points.

Production of CXCL-6, IGF-1, and TGF-β2 was quantified by ELISA (R&D Systems, Minneapolis, MN), according to the manufacturer's instructions. This immunometric assay is based on a quantitative sandwich enzyme immunoassay technique.

2.6. Statistical analysis

The software GraphPad Prism version 5.03 (GraphPad Software, La Jolla, CA) was used for statistical analysis of cytokine data applying two-factor ANOVA or Student's 2-tailed *t*-test, when appropriate. Differences with a *P*-value <0.05 were considered statistically significant.

3. Results

To find which genes were modulated by Aminaphtone in IL1β-stimulated ECV304 endothelial cells at the transcriptional level, we performed supervised analyses that combined an empirical Bayesian approach and a parametric two-factor ANOVA comparing treated *vs.* untreated cells at 1, 3 and 6 h, respectively (Table 1). Two hundred and fifty-two genes were found significantly different with an FDR <0.1 at the BETR test (Table 1 in Ref. Salazar et al., submitted for publication). Two-way ANOVA showed that 139 of these genes were significant for the treatment effect only, 47 genes for the interaction effect only, and 66 genes for both effects. Post-hoc comparisons identified as significantly up- or down-regulated respectively 103 and 80 genes at 1 h treatment, 64 and 53 genes at 3 h, and 35 and 76 genes at 6 h, in Aminaphtone-treated *vs.* untreated ECV304 cells. Unsupervised hierarchical clustering showed that these genes correctly discriminated between time points and treatments (Fig. 1 in Ref. Salazar et al., submitted for publication).

Using a clustering algorithm to identify tight groups (kernels) of highly similar elements among the 252 Aminaphtone-responsive gene transcripts, we identified five clusters of co-regulated genes with different temporal patterns between Aminaphtone-treated and untreated cells (Fig. 1). Cluster_1 contains 83 genes that were significantly upregulated by Aminaphtone at all time points. Cluster_2 contains 69 genes that progressively increase over time, but to a lesser extent in Aminaphtone-treated cells (the net effect is a downregulation at all time points). Cluster_3 contains 44 genes that progressively decrease over time, but to a higher extent in Aminaphtone-treated cells (the net effect is a downregulation at all time points). Cluster_4 contains 32 genes that progressively decrease over time, but to a lesser extent in Aminaphtone-treated cells (the net effect is an upregulation at all time points). Cluster_5 contains 18 genes with an opposite trend between the two treatments.

GO, KEGG, and MSigDB curated gene set comparison on the entire dataset of differentially expressed genes showed that regulation of homeostatic and immune response processes, inflammatory response, cytokine activity, response to hypoxia, cell proliferation, transcription, and cell communication were significantly affected by treatments with Aminaphtone in IL-1β stimulated endothelial cells (Table 2 in Ref. Salazar et al., submitted for publication). Functional analysis of the five gene clusters with similar expression pattern substantially confirmed the aforementioned analysis and showed that the most of variation involving stress and inflammatory responses (including cytokine-cytokine receptor interaction and matrix metalloproteinases) was within Cluster_2 (Table 2), whose genes were on average downregulated at all time points. Consistently, Cluster_3 and Cluster_5 were enriched with genes involved respectively in signal transduction and cell division, which thus turned out to be repressed.

In particular, *EBI3*, *TNFRSF11B* and *TNFSF18* genes, showing a cytokine activity, together with the *EDN1*, *IGFL1*, *CCL22*, and *S100A3* transcripts were found significantly down-regulated at each time-point treatment (see the top differentially expressed genes in Table 1). Incubation with Aminaphtone significantly reduced the IL-1β-induced transcription of a number of proinflammatory cytokines and chemokines: *i.e.* several transcripts showing a cytokine activity, such as the colony stimulating factor 2 and 3 (*CSF2*, *CSF3*), involved in macrophage differentiation, and (C-X-C motif) chemokines and ligands, were found downregulated early after treatment (1 or 3 h; Table 1 and see also Table 1 in Ref. Salazar et al., submitted for publication). *IL1B*, *IL7*, *MMP3*, *MMP10*, and *TGFB2* resulted at lower expression levels at late time points, whereas histone cluster 2 (*HIST2H4A*) was upregulated at all time points.

We then performed a promoter analysis to try and find out TFs whose binding sites are enriched in the promoters of the clusters of co-regulated genes identified above (Table 3). Results showed that at least 12 binding sites are significantly over-represented in the set of promoters of the co-expressed gene clusters. In particular, Aminaphtone putatively influenced the regulation of gene expression through TFs that binds to the TATA-box (the core promoter sequence) in Cluter_2 and through 8 TFs, including zinc finger proteins, in Cluster_3.

Microarray data were confirmed by RT-qPCR on a set of six genes, (*CSF3*, *IGFL1*, *TGFB2*, *TNF*, *TNFRSF11B*, and *TNFSF18*). RT-qPCR and microarray analyses showed a strong correlation, as ascertained by highly significant ($P<0.0001$) Pearson's coefficients (Fig. 2, left column). The original dataset was validated also against

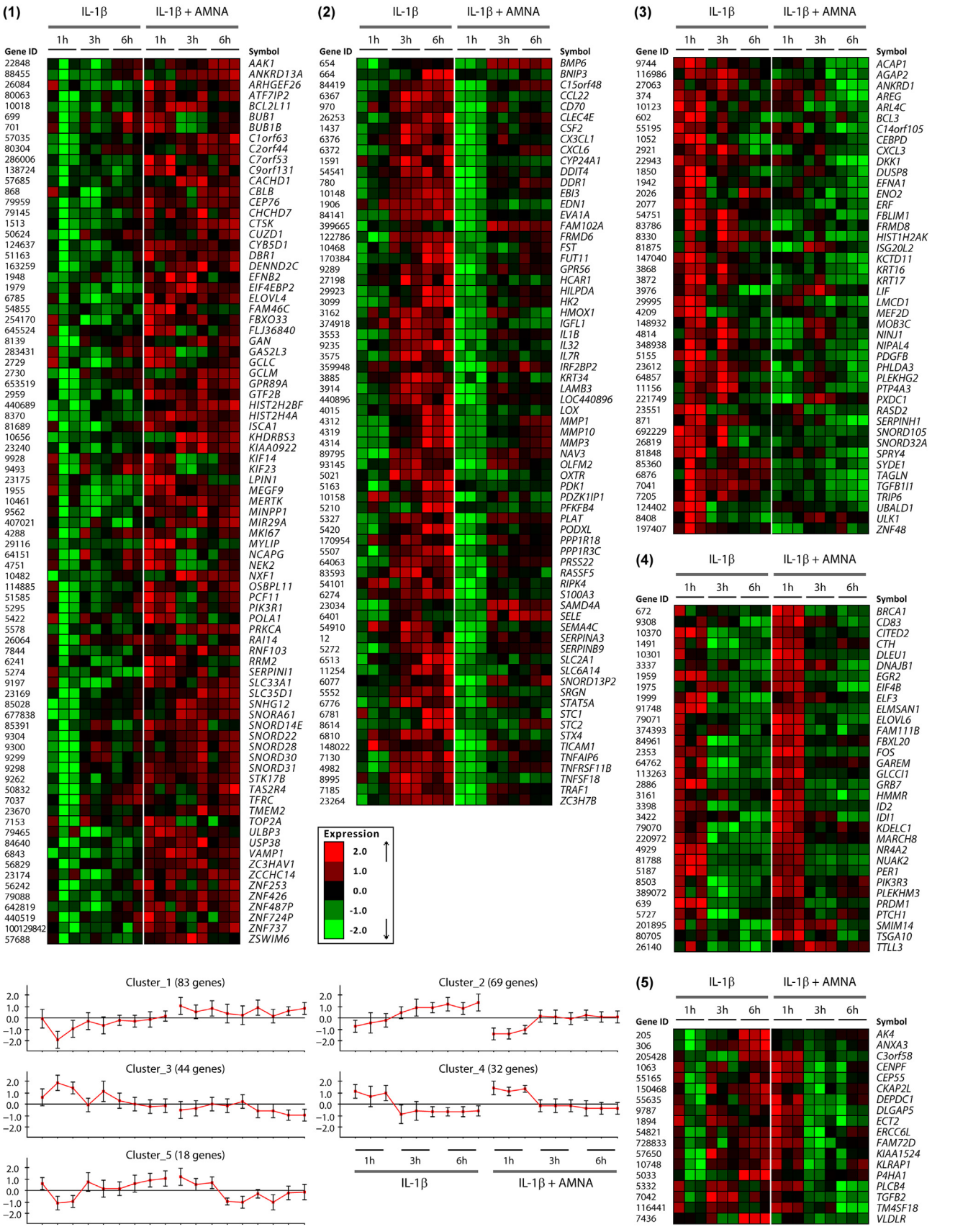

Fig. 1. Heatmaps of differentially expressed genes, as identified by the BETR algorithm, modulated by Aminaphtone (AMNA) in treated *vs.* untreated IL1β-stimulated endothelial cells. The CLICK clustering algorithm identified 5 distinct gene clusters with similar expression patterns. Panels in the bottom left part of the figure show the average expression patterns in the 5 clusters (mean ± S. E. M. of the normalized mean-centred expression values).

Table 2
Biological processes and pathways significantly modulated by Aminaphtone in treated *vs.* untreated IL-1β stimulated endothelial cells.

Set	Enriched with GO term and/or *KEGG pathway*	#genes	*raw* P	*corr.* P	Gene List
Cluster_1	interspecies interaction between organisms	9	6.82E-06	0.0240	*[ULBP3, TFRC, EFNB2, POLA1, BUB1, NXF1, GTF2B, PIK3R1, BCL2L11]*
Cluster_2	cytokine activity	12	3.68E-12	0.0010	*[CSF2, TNFRSF11B, CCL22, EDN1, IL1B, IL32, CD70, CXCL6, CX3CL1, TNFSF18, EBI3, BMP6]*
	response to decreased oxygen levels	11	1.60E-10	0.0010	*[PLAT, STC2, HMOX1, EDN1, BNIP3, IL1B, OXTR, STC1, CX3CL1, MMP3, DDIT4]*
	immune system process	21	2.99E-09	0.0010	*[CSF2, PODXL, STAT5A, FST, EDN1, BNIP3, CD70, IL32, CXCL6, CX3CL1, IL7R, TNFSF18, MMP1, SERPINB9, CCL22, CLEC4E, TICAM1, IL1B, SELE, EBI3, BMP6]*
	response to wounding	17	9.13E-09	0.0010	*[PLAT, STX4, CXCL6, CX3CL1, MMP3, MMP1, DDR1, TNFAIP6, CCL22, HMOX1, TICAM1, SERPINA3, IL1B, LOX, SELE, SRGN, BMP6]*
	response to steroid hormone stimulus	11	1.51E-08	0.0010	*[PLAT, SERPINB9, TNFRSF11B, HMOX1, EDN1, IL1B, OXTR, STC1, LOX, MMP3, HCAR1]*
	response to stress	26	7.76E-08	0.0010	*[EDN1, BNIP3, OXTR, IL32, CXCL6, CX3CL1, MMP3, MMP1, CCL22, HMOX1, SLC2A1, TICAM1, SERPINA3, IL1B, LOX, SRGN, PLAT, STX4, STC2, HILPDA, DDIT4, DDR1, TNFAIP6, STC1, SELE, BMP6]*
	negative regulation of secretion	7	9.83E-08	0.0010	*[HMOX1, EDN1, FST, IL1B, OXTR, CX3CL1, SRGN]*
	cell-cell signalling	15	1.33E-07	0.0010	*[PLAT, STX4, STC2, EDN1, OXTR, HILPDA, CD70, CX3CL1, CXCL6, TNFSF18, TNFAIP6, CCL22, GPR56, IL1B, STC1]*
	regulation of cytokine production	10	2.46E-07	0.0020	*[CSF2, CLEC4E, STAT5A, HMOX1, TICAM1, IL1B, HILPDA, CX3CL1, EBI3, SRGN]*
	response to organic substance	19	1.56E-06	0.0070	*[PLAT, STC2, STAT5A, EDN1, OXTR, CX3CL1, IL7R, MMP3, TNFSF18, SERPINB9, TNFRSF11B, HMOX1, TICAM1, IL1B, STC1, LOX, SELE, EBI3, HCAR1]*
	response to cytokine stimulus	10	4.87E-06	0.0180	*[STAT5A, EDN1, IL1B, OXTR, CX3CL1, IL7R, MMP3, TNFSF18, SELE, EBI3]*
	positive regulation of developmental process	11	5.90E-06	0.0210	*[CSF2, STAT5A, HMOX1, EDN1, FST, BNIP3, IL1B, OXTR, CX3CL1, IL7R, BMP6]*
	regulation of localization	16	6.74E-06	0.0230	*[PODXL, FST, EDN1, HK2, OXTR, HILPDA, CX3CL1, MMP3, MMP10, CLEC4E, HMOX1, SLC2A1, IL1B, SELE, SRGN, BMP6]*
	anti-apoptosis	7	8.58E-06	0.0300	*[SERPINB9, CSF2, STAT5A, HMOX1, BNIP3, IL1B, TNFSF18]*
	response to external stimulus	14	8.76E-06	0.0300	*[CYP24A1, STC2, STAT5A, EDN1, BNIP3, CX3CL1, CXCL6, MMP3, TNFRSF11B, CCL22, HMOX1, SLC2A1, IL1B, STC1]*
	regulation of body fluid levels	10	1.50E-05	0.0450	*[PLAT, DDR1, STX4, STAT5A, EDN1, HK2, OXTR, CX3CL1, MMP1, SRGN]*
	Cytokine-cytokine receptor interaction	9	2.5E-07	0.0001	*[CSF2, TNFRSF11B, CCL22, IL1B, CD70, CXCL6, CX3CL1, IL7R, TNFSF18]*
	Matrix Metalloproteinases	3	1.44E-04	0.0052	*MMP10, MMP3, MMP1*
Cluster_3	regulation of signal transduction	16	1.48E-07	0.0010	*[PDGFB, EFNA1, LMCD1, ANKRD1, SPRY4, LIF, PLEKHG2, DKK1, ULK1, SYDE1, ACAP1, TGFB1I1, PHLDA3, AGAP2, DUSP8, RASD2]*
Cluster_4	response to organic substance	12	3.73E-06	0.0110	*[EIF4B, FOS, CD83, CTH, EGR2, NR4A2, PTCH1, DNAJB1, IDI1, PIK3R3, BRCA1, CITED2]*
	negative regulation of macromolecule biosynthetic process	9	3.81E-06	0.0120	*[ELF3, ID2, PER1, PTCH1, MARCH8, PRDM1, GRB7, BRCA1, CITED2]*
Cluster_5	cell division	5	1.59E-05	0.0450	*[CENPF, CEP55, ECT2, ERCC6L, TGFB2]*

GO: Gene Ontology; KEGG: Kyoto Encyclopaedia of Genes and Genomes; Cluster_n: gene clusters identified by the CLICK algorithm; *raw* P: uncorrected *P*-values; *corr.* P: *P*-values corrected for multiple comparisons.

an independent experimental series performed in triplicate, which shown similar results both for transcripts modulated by Aminaphtone at all time points (*CSF3*, *IGFL1*, and *TNFSF18*), and for genes modulated at late time points (*TGFB2* and *TNFRSF11B*), or for an unmodulated transcript such as *TNF* (see Table 1 and Fig. 2, right column).

A multiplex ELISA experiment confirmed and extended the observations described above. We analysed at different time points (3, 6, 12, and 24 h) the release of a total of 30 cytokines and chemokines. We found that 21 out of 30 were detectable in the supernatants. Two-way ANOVA (Table 4), followed by Bonferroni pairwise comparison (Fig. 3), showed that 15 chemokines/cytokines were significantly modulated by Aminaphtone, namely: CCL2 (MCP-1), CSF2 (GM-CSF), CSF3 (G-CSF), CXCL10 (IP-10), IFNA1 (IFN-α), TNF (TNF-α), IL1R1 (IL-1RA), IL-6, IL-7, IL-8, IL-10, IL-15, EGF, FGF2 (FGF-basic), VEGFA (VEGF). All appeared to be downregulated except FGF2, which was upregulated at early time points (Fig. 3).

We further extended our observations by analysing with an immunoassay quantitative technique three additional proteins (Fig. 4). CXCL6 and TGF-β2 production showed a down-modulation with a high statistical significance at late time points (12 and 24 h). Finally, IGF1 production was upregulated by Aminaphtone at all time points.

Consistent with these results, most of the chemokines and cytokines that were found downregulated at the protein level in the supernatants (Figs. 3 and, 4) appeared to be significantly downregulated at the mRNA level (Table 5): *i.e.*, CCL2, CSF2, CSF3, CXCL6, IL-6, TGF-β2, and VEGF. In addition, IL-8 mRNA and protein were not significantly modulated by Aminaphtone at any time point, even if the protein showed a trend in downregulation. On the contrary, TNF-α was strongly downregulated at protein but not at mRNA level: this suggests that the drug had also post-transcriptional effects. This may be the case also for IL1R1 and FGF2, which did not show any significant regulation at the mRNA level. We could not perform this comparison for the other 8 cytokines, because their signals on the microarray were too low or did not pass the quality control criteria.

4. Discussion

The main finding of this study is that Aminaphtone showed many unexpected biological activities, which may potentially be effective in the therapeutic management of several inflammatory diseases. Previous works analysed the effects of Aminaphtone in the treatment of CVI, which is the clinical condition the drug is mainly used for. The results of this study showed remarkable downregulation of an array of inflammatory molecules and upregulation of genes protective against the inflammatory state. Indeed, Aminaphtone was capable of down-regulating both at the mRNA and the protein level the majority of molecules across the

Table 3
Promoter analysis in gene clusters modulated by Aminaphtone in treated *vs.* untreated IL1β-stimulated endothelial cells.

Gene set	Enriched with TF binding sites	#genes	*P*	Gene List
Cluster_1	M88819 [Rubin-10 (MTE)]	28	2.64E-04	*RAI14(−84,−7), NCAPG(−174), PRKCA(−719), CYB5D1(63), VAMP1(−17), CBLB(166), STK17B(−79,135), ZC3HAV1 (152), GCLC(175), LPIN1(−44), ZCCHC14(−948), ZNF426(−23), SLC33A1(153), EIF4EBP2(−118), ISCA1(−471), BCL2L11(−331,−204,167), MERTK(−444), AAK1(−557,20), EFNB2(−499), GCLM(−246), C7orf53(−313), CACHD1 (−462), MKI67(−109,−51), OSBPL11(−667,−125), SERPINI1(192), GAS2L3(40), KIAA0922(−186,10), PIK3R1(162)*
Cluster_2	M00043 [dl]	14	9.16E-06	*TlCAM1(−107), SLC6A14(−493,−127), OLFM2(−385), CD70(−55), DDIT4(−973), CCL22(−222), CXCL6(91), EBI3 (−295), PLAT(−500), HILPDA(−393), IL1B(−172), FRMD6(−298), NAV3(−328), SAMD4A(−298)*
	M00216 [TATA]	11	5.25E-05	*MMP3(−812,162), ZC3H7B(−177), MMP10(−33), SELE(−295,−49), KRT34(−373), FRMD6(−779), CLEC4E(−730), NAV3(−428,159), SAMD4A(52), LOX(−468,−421), IL7R(−554)*
Cluster_3	M00720 [CAC-binding protein]	21	3.14E-08	*TRIP6(−709,−88), PDGFB(−49), AGAP2(−121), KCTD11(−872), SPRY4(−433), ANKRD1(99), SYDE1(−291), EFNA1 (−588), ERF(−191), ZNF48(−757,−462), ACAP1(−70), ISG20L2(104), PHLDA3(−408,−319), TAGLN(−70), LIF (−852,−618,−81), NINJ1(−603), ARL4C(−571,−477), SERPINH1(−696,−88,149), FBLIM1(−519), BCL3 (−619,−608), MOB3C(−881,−826,−339)*
	M00915 [AP-2]	21	4.54E-05	*TRIP6(−948), MEF2D(−444), KCTD11(−870), RASD2(−494), DUSP8(−682,−643), SPRY4(−971,−518), KRT16 (−343), SYDE1(−184,−12), EFNA1(−625), ERF(−687), ZNF48(−152,−107), ACAP1(67), UBALD1 (−859,−305,−15), TGFB1I1(−90), PHLDA3(−235), NINJ1(−744,−86), ARL4C(187), PTP4A3(−196), ENO2(−232), SERPINH1(−93,39), PLEKHG2(−21)*
	M00257 [RREB-1]	19	5.79E-05	*TRIP6(−880), MEF2D(−162), PDGFB(−911), NIPAL4(−956), KCTD11(−878), DKK1(−610,−144), KRT16(−206), SYDE1(−455), EFNA1(−920,−113), ERF(−677,−483,−203), ZNF48(−463), ACAP1(−897), TGFB1I1(−241), TAGLN (−375), LIF(−82), NINJ1(−609), FBLIM1(−545,−536,−525), BCL3(−614), MOB3C(−338,−134)*
	M00401 [ABF1]	15	1.95E-04	*TRIP6(71), MEF2D(−453,−439,−110), PXDC1(105,114), KCTD11(−468,−230,−142), DUSP8(−698,−677,−661), FRMD8(−991,−125,81), RASD2(−712,−20), EFNA1(−725), ERF(−69,−58), ISG20L2(−844,128), TGFB1I1(−55,12), ENO2(45), PTP4A3(−40,176), SERPINH1(−37), PLEKHG2(74)*
	jMA0056 [ZNF42 1–4]	35	2.95E-04	*TRIP6(−851,−704,−325,−229,54), MEF2D(−774,−121), RASD2(−988,−141), KRT16 (−899,−448,−435,−339,−263,−55), ANKRD1(−779), ERF(−683,−632,−591,−562,−387), ZNF48(−487), UBALD1(−302,−44), TGFB1I1(−5), PHLDA3(−786,−646), LMCD1(−132), ENO2(96), PTP4A3(−585,−58), BCL3 (−894,−621,−126), PXDC1(−461), ULK1(−751), PDGFB(−434), AGAP2(−687), NIPAL4(−76), KCTD11(−676), C14orf105(−509), DUSP8(−982,−821,105), DKK1(73), CXCL3(−438,−9), SPRY4(−499), SYDE1(−494,−478,−439), EFNA1(−83), ACAP1(54,153), TAGLN(−982,−776,−376,−349,−110,−65,115), LIF (−973,−873,−792,−620,−285,−83,10,79), ARL4C(−457,−260,191), SERPINH1(−415,−43,154), FBLIM1 (−588,−402), PLEKHG2(−430), MOB3C(−876,−706,−329,−125,−29)*
	M01033 [HNF4]	28	3.95E-04	*TRIP6(−532), MEF2D(−742,−303), RASD2(−379,−207,117), KRT16(−908,−887,−376), ERF (−817,−504,−394,−282), UBALD1(−819,−784,−675,−210), ENO2(−395,−349,66), PTP4A3(−213,−194,−35), BCL3(−917,−686,−666,−499,−45), PXDC1(−338,−264), ULK1(−278), NIPAL4(−117,−7,96), KCTD11(−900), FRMD8(103), DUSP8(−459,119), DKK1(−393), CXCL3(−239), SPRY4(−509,96), EFNA1(−77,21), ISG20L2(178), ACAP1(−875,−10,68), TAGLN(−337), LIF(−355,−330), NINJ1(−612,−50), ARL4C(−783,−736,−416,−334), FBLIM1(−635), SERPINH1(−165), MOB3C(−109,24)*
	M01122 [ZNF219]	19	4.40E-04	*PXDC1(−823,−812,−645), MEF2D(−578,−12), PDGFB(189), DUSP8(−521), SPRY4(−856,−431), KRT16(−989), EFNA1(−49), ERF(−195,−38), ZNF48(−460,−347), ISG20L2(−490), UBALD1(−366), TGFB1I1(63), LIF(−75), NINJ1 (−538), LMCD1(−726), FBLIM1(−285), PLEKHG2(−26), BCL3(−606), MOB3C(−886)*
	M00002 [E47]	14	4.89E-04	*PXDC1(−777,−715), KCTD11(−339), RASD2(−327), SPRY4(−338), KRT16(−924), ANKRD1(−101), EFNA1(−835), ERF(−699,−513), PHLDA3(−377), CEBPD(−738), NINJ1(−663), LMCD1(94), ARL4C(−931), FBLIM1(44)*
Cluster_4	M00725 [HP1 site factor]	7	3.51E-04	*PRDM1(−540), EGR2(168), NR4A2(−613), BRCA1(−605,−455), MARCH8(−132), ELOVL6(−921), GLCCI1 (−941,−755)*

TF: transcription factor; binding sites, in square brackets, are identified by their BIOBASE accession number.
MTE: motif ten element; dl: dorsal; Ap-2: activating protein 2; RREB1: RAS-responsive element binding protein 1; ABF1: activated B cell factor-1; ZNF42: zinc finger protein 42; HNF4: hepatocyte nuclear factor 4; ZNF219: zinc finger protein 219; HP1: heterochromatin protein 1.
The gene lists contain the position of the TF binding site for a given gene.

entire inflammatory panel induced by stimulation with IL-1β. Likewise, we documented an upregulation of an antiinflammatory factor such as IGF1.

Aminaphtone appeared also able to favourably modulate immune response genes (down-regulating cytokine biosynthesis, transcripts involved in lymphocyte differentiation and cell proliferation, and cytokine-cytokine receptor interaction) and to regulate genes engaged in homeostasis, secretion, body fluid levels, response to hypoxia, cell division, and cell-to-cell communication and signalling. Results were confirmed and extended analysing the secretome of endothelial cells at different time points after stimulation with IL-1β, showing significant reduction of the release of 14 cytokines and chemokines. Most of these latter effects were confirmed at the transcriptional level. Conversely, some effects, in particular the downregulation of TN-α, appeared to be at post-transcriptional level, thus indicating that the drug may act at multiple stages.

Using graph-theoretic and statistical techniques, we identified five clusters of highly similar expressed genes. Assuming that genes co-expressed over multiple time points are regulated by common TFs, and therefore are expected to share common regulatory elements in their promoters, we identified TFs whose binding sites are significantly over-represented in those gene clusters, based on known models for TF binding sites. Using this approach, we predicted several TFs as highly significant candidate regulators of the corresponding set of Aminaphtone-responsive genes. The picture that emerges is very complex and may include interactions with TFs involved in angiogenesis, such as zinc finger proteins (Hamik et al., 2006), in cell cycle, such as the basic helix-loop-helix TF E47 (Kim et al., 2015), and in proliferation and differentiation, such as AP-2 (Eckert et al., 2005). Interestingly, promoters of genes in Cluster_2 are enriched with binding sites for Dorsal, a Rel-protein with activator/repressor functions that is the Drosophila homolog of mammalian NF-κB (Mrinal et al., 2011),

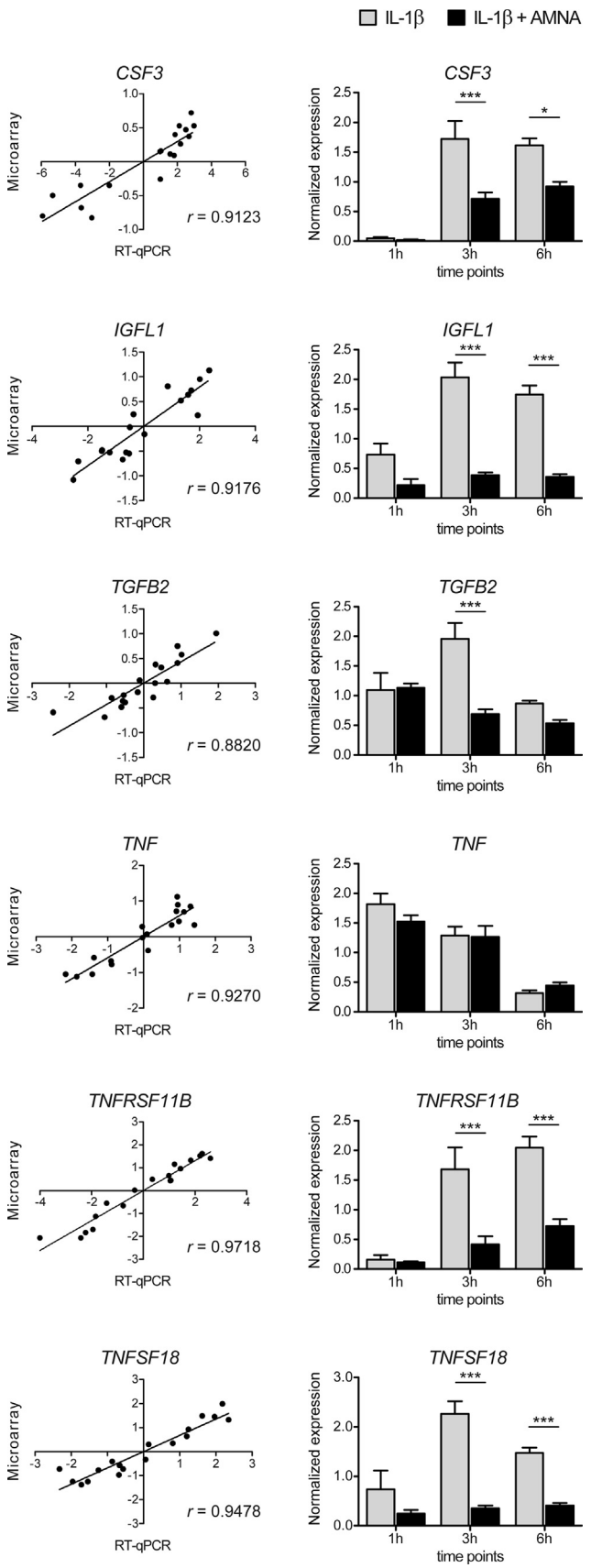

Fig. 2. RT-qPCR confirmation (left column) and validation on an independent experiment (right column) of gene expression in Aminaphtone-treated *vs.* untreated IL1β-stimulated endothelial cells. All Pearson's correlation coefficient has a *P*-value < 0.0001.

Table 4
Chemokines and cytokines modulated by Aminaphtone in treated *vs.* untreated IL1β-stimulated endothelial cells.

	Source of Variation	CCL2	CSF2	CSF3	CXCL10	IFN-α	TNF-α	IL-1RA	IL-6	IL-7	IL-8	IL-10	IL-15	EGF	FGF2	VEGF
P-value	Interaction	0.0061	< 0.0001	< 0.0001	0.0371	0.2073	0.0067	0.0454	0.4474	0.0975	0.8389	0.9927	0.1957	0.1709	0.0221	0.2566
	Drug	**< 0.0001**	**< 0.0001**	**< 0.0001**	**< 0.0001**	**< 0.0001**	**< 0.0001**	**0.0092**	**0.0004**	**0.0009**	**0.0238**	**0.0022**	**0.0002**	**0.0100**	**0.0439**	**0.0024**
	Time	< 0.0001	< 0.0001	< 0.0001	0.0003	< 0.0001	0.0001	< 0.0001	< 0.0001	0.0003	< 0.0001	0.0311	< 0.0001	0.0073	< 0.0001	< 0.0001
% total variance	Interaction	6.47	5.87	4.33	7.02	1.37	9.89	4.50	1.70	8.12	0.60	0.16	2.37	7.38	5.81	3.47
	Drug	21.85	16.47	9.84	55.71	8.13	39.95	4.73	9.67	15.39	3.95	19.49	8.34	15.00	2.19	8.86
	Time	53.61	75.03	80.27	27.66	78.96	22.11	81.21	71.28	28.83	70.77	17.73	70.04	23.23	84.68	57.79

P-values for the interaction, treatment, and time effects at two-factor. ANOVA.

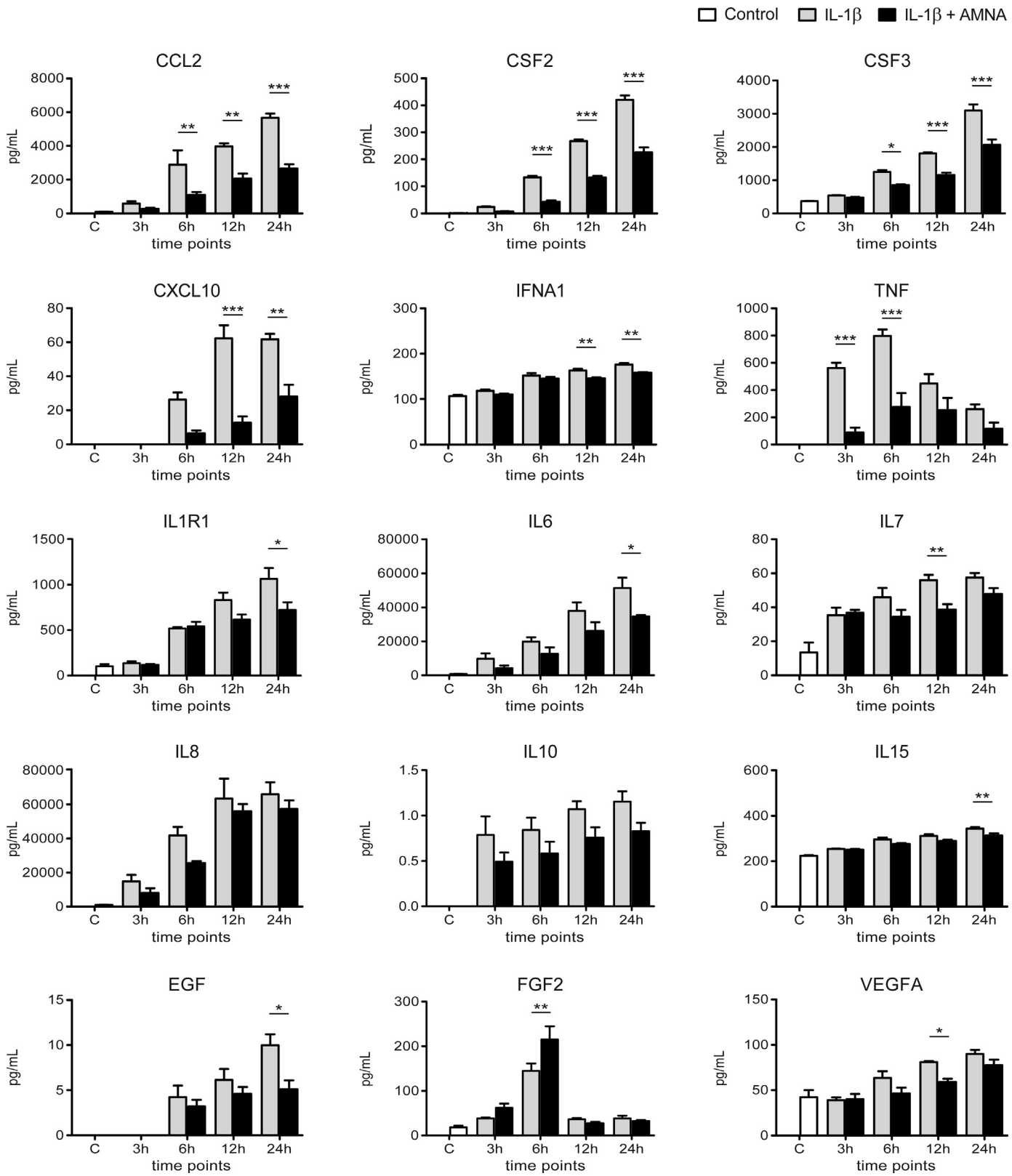

Fig. 3. Multiplex cytokine/chemokine analysis of the secretome of Aminaphtone-treated *vs.* untreated IL1β-stimulated endothelial cells (n = 6 for each treatment). $^{*}P < 0.05$, $^{**}P < 0.01$, $^{***}P < 0.001$.

and with TATA-box DNA sequence, which is bound by a number of TFs to make up the RNA polymerase II preinitiation complex (Lee and Young, 2000): these TFs have both been shown to interact with several inflammatory and immune regulators. Further studies are needed to dissect the molecular mechanism of action of Aminaphtone.

Focussing our attention on inflammation-related genes, the effect of Aminaphtone appears as a substantial and coordinated

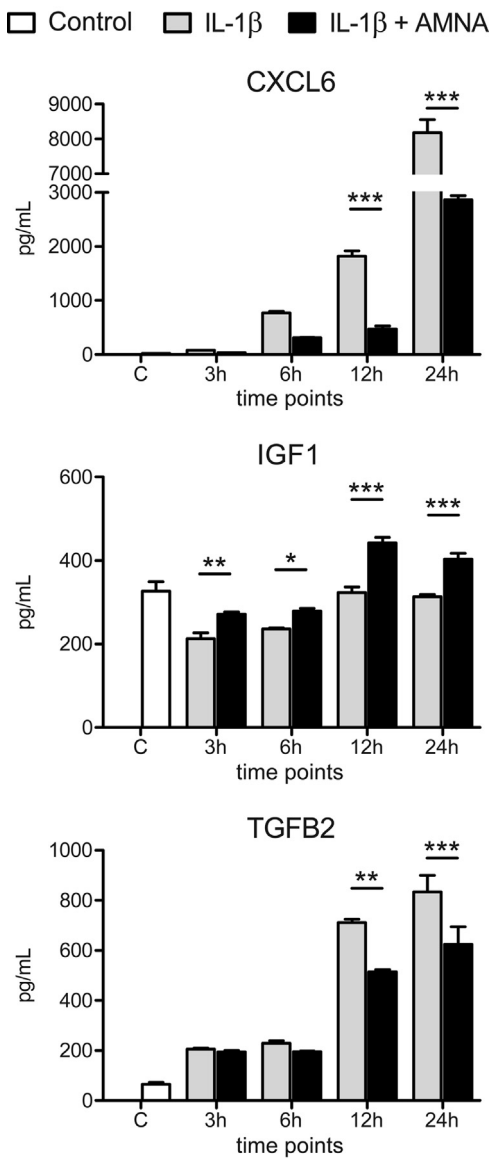

Fig. 4. ELISA analysis of CXCL6, IGF-1, and TGF-β2 release by Aminaphtone-treated *vs.* untreated IL1β-stimulated endothelial cells (n=6 for each treatment). * $P<0.05$, ** $P<0.01$, *** $P<0.001$.

influence on the inflammatory state of the endothelial cells stimulated by IL1β, which can be divided in several phases: (1) early and sustained downregulation of vasoactive and inflammatory genes (EDN1, HMOX1, EBI3, and TRAF1), consistent with our previous observations (Scorza et al., 2008a). In particular, EBI3 encodes a secreted that heterodimerizes with a 28 kDa protein to form interleukin 27, a cytokine that regulates T cell and inflammatory responses in part by activating the Jak/STAT pathway. (2) Early but transient downregulation of inflammatory factors (SERPINA3, PDGFB, CXCL3) and the stress-response nuclear receptor NR4A2. Dysregulation of the latter gene has been associated with rheumatoid arthritis (Smith, 2001). (3) A late downregulation of AREG, a member of the epidermal growth factor family, and a late downregulation of IL1β, and the matrix metallopeptidase MMP3. The protein encoded by AREG interacts with the EGF/TGF-α receptor to promote the growth of normal epithelial cells and is associated with a psoriasis-like skin phenotype (Pereira de Godoy, 2008). (4) An early and sustained upregulation of PRKCA, a kinase that plays roles in many different cellular processes, such as cell adhesion, cell transformation, cell cycle checkpoint, and cell volume control, as well as vasoreactivity (de Godoy and Batigalia, 2009). (5) Early but transient upregulation of CD83, BRCA1, and of the transcription factor FOS. Reduced expression of FOS has been associated to impaired vasculogenesis (Hamik et al., 2006).

These findings are particularly intriguing, because of the possible use of this drug in diseases where cytokine activation, vasoconstriction, fibrosis, and endothelial damage play a central role. This observation prompts for further studies aimed at investigating whether Aminaphtone may act like a broad spectrum anti-inflammatory drug.

Noteworthy effects of Aminaphtone are those on TGF-β2, CXCL6, and IGF-1 release. TGFβ2 is one of the main molecules active in inflammatory mechanism with a role in fibrotic process. In particular its production is very increased in patients with systemic sclerosis (Falanga et al., 1992; Hasegawa et al., 2004; Leask, 2006). In this light, the decrement of its release by IL1β-stimulated endothelial cells lately after treatment with Aminaphtone appears of great importance. CXCL-6 is a chemotactic factor (Wuyts et al., 2003) involved in the neutrophil recruitment in the site of venous ulcer in CVI. The significant down-regulation of its mRNA and protein release induced by Aminaphtone may, at least in part, explain the drug effectiveness in this pathologic condition. IGF-1, the insulin growth factor 1, exerts pleiotropic antioxidant and anti-inflammatory effects, which together may reduce atherosclerotic burden and vascular injury (Shai et al., 2011), and has a protective role in the pulmonary fibrotic process. High IGF-1 levels are, in fact, dosed in patients affected by idiopathic pulmonary fibrosis and are correlated with a better healing because of its property in the induction of epithelialization repair in post-inflammation tissue (Krein and Winston, 2002; Muguerza et al., 2001). Thus, IGF-1 up-regulation induced by Aminaphtone

Table 5
Difference in expression at the mRNA level of chemokines and cytokines modulated by Aminaphtone in treated *vs.* untreated IL1β-stimulated endothelial cells.

		Fold-change			*Pairwise significant*		
Symbol	**Name**	**1 h**	**3 h**	**6 h**	***1 h***	***3 h***	***6 h***
CCL2	chemokine (C-C motif) ligand 2	−1.5	−1.1	−1.1	a		
CSF2	colony stimulating factor 2 (granulocyte-macrophage)	−1.7	−1.9	−1.5	a	b	
CSF3	colony stimulating factor 3 (granulocyte)	−1.2	−1.4	−1.2		a	
CXCL6	chemokine (C-X-C motif) ligand 6	−1.4	−1.3	−1.6	a	a	b
FGF2	fibroblast growth factor 2 (basic)	1.3	−1.3	−1.1			
IL1R1	interleukin 1 receptor, type I	1.7	1.5	1.4			
IL6	interleukin 6 (interferon, beta 2)	−1.4	−1.3	−1.1	a		
IL8	interleukin 8	1.0	−1.1	−1.1			
TGFB2	transforming growth factor, beta 2	1.2	−2.1	−1.5		b	a
TNF	tumor necrosis factor	−1.2	1.2	1.3			
VEGFA	vascular endothelial growth factor A	−1.2	−1.3	−1.4			a

Pairwise significant: significance level for pairwise comparisons: [a] $P<0.05$; [b] $P<0.01$.

could have a therapeutic role in many inflammatory disorders, as it is shown to be a protective anti-fibrotic factor.

As a matter of speculation, it is therefore possible to imagine a role of Aminaphtone in the treatment of those clinical conditions in which the endothelial damage is a key event and/or precedes all other manifestations. An example of this is systemic sclerosis, a disease in which molecules like TGF-β and several other inflammatory proteins are strongly involved (Gruschwitz et al., 1990). Another example is pulmonary hypertension, which remains one of the most terrible complications of systemic sclerosis, in which a key role is exerted by endothelin-1 (Chester and Yacoub, 2014; Santaniello et al., 2006). Finally, another paramount example is atherosclerosis and related conditions, of which the endothelial dysfunction is an early marker (Davignon and Ganz, 2004). The underlying idea is to use Aminaphtone as a novel treatment in pathologies in which chronic inflammatory state and endothelium dysfunction are the main pathogenic features.

Financial support

The work was entirely supported by internal funds from the Fondazione IRCCS Ca' Granda Ospedale Maggiore Policlinico, Milano, Italy. The drug was kindly provided by Laboratori Baldacci S. p. A. (Via S. Michele degli Scalzi, 73, 56124 Pisa, Italy), which had no part in the study design, data analysis, and drafting of the present manuscript.

Acknowledgments

The authors gratefully acknowledge Elena Grovetti (Department of Pathophysiology and Transplantation, Università degli Studi di Milano) for excellent technical assistance.

References

Andersen, C.L., Jensen, J.L., Orntoft, T.F., 2004. Normalization of real-time quantitative reverse transcription-PCR data: a model-based variance estimation approach to identify genes suited for normalization, applied to bladder and colon cancer data sets. Cancer Res. 64, 5245–5250.

Aryee, M.J., Gutierrez-Pabello, J.A., Kramnik, I., Maiti, T., Quackenbush, J., 2009. An improved empirical bayes approach to estimating differential gene expression in microarray time-course data: BETR (Bayesian Estimation of Temporal Regulation). BMC Bioinforma. 10, 409.

Bolstad, B.M., Irizarry, R.A., Astrand, M., Speed, T.P., 2003. A comparison of normalization methods for high density oligonucleotide array data based on variance and bias. Bioinformatics 19, 185–193.

Chester, A.H., Yacoub, M.H., 2014. The role of endothelin-1 in pulmonary arterial hypertension. Glob. Cardiol. Sci. Pract. 2014, 62–78.

Davignon, J., Ganz, P., 2004. Role of endothelial dysfunction in atherosclerosis. Circulation 109, III27–32.

Doni, A., Mondaini, F., Somigli, M., Comparini, L., Gavazzi, M., Ventimiglia, V., 1983. Modification of primary hemostasis and capillary fragility induced by aminaftone in chronic renal insufficiency. Clin. Ter. 107, 45–50.

Eckert, D., Buhl, S., Weber, S., Jager, R., Schorle, H., 2005. The AP-2 family of transcription factors. Genome Biol. 6, 246.

Falanga, V., Gerhardt, C.O., Dasch, J.R., Takehara, K., Ksander, G.A., 1992. Skin distribution and differential expression of transforming growth factor beta 1 and beta 2. J. Dermatol. Sci. 3, 131–136.

Gentleman, R.C., Carey, V.J., Bates, D.M., Bolstad, B., Dettling, M., Dudoit, S., Ellis, B., Gautier, L., Ge, Y., Gentry, J., Hornik, K., Hothorn, T., Huber, W., Iacus, S., Irizarry, R., Leisch, F., Li, C., Maechler, M., Rossini, A.J., Sawitzki, G., Smith, C., Smyth, G., Tierney, L., Yang, J.Y., Zhang, J., 2004. Bioconductor: open software development for computational biology and bioinformatics. Genome Biol. 5, R80.

Giaid, A., Yanagisawa, M., Langleben, D., Michel, R.P., Levy, R., Shennib, H., Kimura, S., Masaki, T., Duguid, W.P., Stewart, D.J., 1993. Expression of endothelin-1 in the lungs of patients with pulmonary hypertension. N. Engl. J. Med. 328, 1732–1739.

de Godoy, J.M., Batigalia, F., 2009. Aminaphtone in the control of Schamberg's disease. Thromb. J. 7, 8.

Gruschwitz, M., Muller, P.U., Sepp, N., Hofer, E., Fontana, A., Wick, G., 1990. Transcription and expression of transforming growth factor type beta in the skin of progressive systemic sclerosis: a mediator of fibrosis? J. Invest. Dermatol. 94, 197–203.

Hamik, A., Wang, B., Jain, M.K., 2006. Transcriptional regulators of angiogenesis. Arterioscler. Thromb. Vasc. Biol. 26, 1936–1947.

Hasegawa, M., Sato, S., Takehara, K., 2004. Augmented production of transforming growth factor-beta by cultured peripheral blood mononuclear cells from patients with systemic sclerosis. Arch. Dermatol. Res. 296, 89–93.

Irizarry, R.A., Hobbs, B., Collin, F., Beazer-Barclay, Y.D., Antonellis, K.J., Scherf, U., Speed, T.P., 2003. Exploration, normalization, and summaries of high density oligonucleotide array probe level data. Biostatistics 4, 249–264.

Kim, S., Lahmy, R., Riha, C., Yang, C., Jakubison, B.L., van Niekerk, J., Staub, C., Wu, Y., Gates, K., Dong, D.S., Konieczny, S.F., Itkin-Ansari, P., 2015. The basic helix-loop-helix transcription factor E47 reprograms human pancreatic cancer cells to a quiescent acinar state with reduced tumorigenic potential. Pancreas 44, 718–727.

Krein, P.M., Winston, B.W., 2002. Roles for insulin-like growth factor I and transforming growth factor-beta in fibrotic lung disease. Chest 122, 289S–293S.

Leask, A., 2006. Scar wars: is TGFbeta the phantom menace in scleroderma? Arthritis Res. Ther. 8, 213.

Lee, T.I., Young, R.A., 2000. Transcription of eukaryotic protein-coding genes. Annu. Rev. Genet. 34, 77–137.

Mrinal, N., Tomar, A., Nagaraju, J., 2011. Role of sequence encoded kappaB DNA geometry in gene regulation by Dorsal. Nucleic Acids Res. 39, 9574–9591.

Muguerza, B., Castilla-Cortazar, I., Garcia, M., Quiroga, J., Santidrian, S., Prieto, J., 2001. Antifibrogenic effect *in vivo* of low doses of insulin-like growth factor-I in cirrhotic rats. Biochim. Biophys. Acta 1536, 185–195.

Pereira de Godoy, J.M., 2008. Aminaphtone in idiopathic cyclic oedema syndrome. Phlebology 23, 118–119.

Pfaffl, M.W., 2001. A new mathematical model for relative quantification in real-time RT-PCR. Nucleic Acids Res. 29, e45.

Saeed, A.I., Sharov, V., White, J., Li, J., Liang, W., Bhagabati, N., Braisted, J., Klapa, M., Currier, T., Thiagarajan, M., Sturn, A., Snuffin, M., Rezantsev, A., Popov, D., Ryltsov, A., Kostukovich, E., Borisovsky, I., Liu, Z., Vinsavich, A., Trush, V., Quackenbush, J., 2003. TM4: a free, open-source system for microarray data management and analysis. Biotechniques 34, 374–378.

Salazar, G., Bellocchi, C., Todoerti, K., Saporiti, F., Piacentini, L., Scorza, R., Colombo, G.I., 2016. Time-course gene expression data on the transcriptional effects of Aminaphtone on ECV304 endothelial cells. Data Brief. (submitted for publication)

Santaniello, A., Salazar, G., Lenna, S., Antonioli, R., Colombo, G., Beretta, L., Scorza, R., 2006. HLA-B35 upregulates the production of endothelin-1 in HLA-transfected cells: a possible pathogenetic role in pulmonary hypertension. Tissue Antigens 68, 239–244.

Scorza, R., Santaniello, A., Salazar, G., Lenna, S., Colombo, G., Turcatti, F., Beretta, L., 2008a. Aminaftone, a derivative of 4-aminobenzoic acid, downregulates endothelin-1 production in ECV304 Cells: an *in vitro* Study. Drugs R. D. 9, 251–257.

Scorza, R., Santaniello, A., Salazar, G., Lenna, S., Della Bella, S., Antonioli, R., Toussoun, K., Beretta, L., 2008b. Effects of aminaftone 75 mg TID on soluble adhesion molecules: a 12-week, randomized, open-label pilot study in patients with systemic sclerosis. Clin. Ther. 30, 924–929.

Shai, S.Y., Sukhanov, S., Higashi, Y., Vaughn, C., Rosen, C.J., Delafontaine, P., 2011. Low circulating insulin-like growth factor I increases atherosclerosis in ApoE-deficient mice. Am. J. Physiol. Heart Circ. Physiol. 300, H1898–H1906.

Sharan, R., Maron-Katz, A., Shamir, R., 2003. CLICK and EXPANDER: a system for clustering and visualizing gene expression data. Bioinformatics 19, 1787–1799.

Smith, P.D., 2001. Update on chronic-venous-insufficiency-induced inflammatory processes. Angiology 52 (Suppl. 1), S35–S42.

Subramanian, A., Tamayo, P., Mootha, V.K., Mukherjee, S., Ebert, B.L., Gillette, M.A., Paulovich, A., Pomeroy, S.L., Golub, T.R., Lander, E.S., Mesirov, J.P., 2005. Gene Set enrichment Analysis: A Knowledge-based Approach for interpreting Genome-Wide Expression profiles. Proc. Natl. Acad. Sci. U. S. A. 102, 15545–15550.

Supek, F., Bosnjak, M., Skunca, N., Smuc, T., 2011. REVIGO summarizes and visualizes long lists of gene ontology terms. PLoS One. 6, e21800.

The Gene Ontology Consortium, 2015. Gene Ontology Consortium: going forward. Nucleic Acids Res. 43, D1049–D1056.

Villaverde, C.A., Hernandez, R., Santolaya, C., 1989. Vascular Permeability Modification by aminaftone. Rev. Pharmacol. Clin. Exp. 6, 9–14.

Wingender, E., 2008. The TRANSFAC project as an example of framework technology that supports the analysis of genomic regulation. Brief Bioinform. 9, 326–332.

Wuyts, A., Struyf, S., Gijsbers, K., Schutyser, E., Put, W., Conings, R., Lenaerts, J.P., Geboes, K., Opdenakker, G., Menten, P., Proost, P., Van Damme, J., 2003. The CXC chemokine GCP-2/CXCL6 is predominantly induced in mesenchymal cells by interleukin-1beta and is down-regulated by interferon-gamma: comparison with interleukin-8/CXCL8. Lab. Invest. 83, 23–34.

Zambelli, V., Santaniello, A., Fumagalli, F., Masson, S., Scorza, R., Beretta, L., Latini, R., 2011. Efficacy of aminaftone in a rat model of monocrotaline-induced pulmonary hypertension. Eur. J. Pharmacol. 667, 287–291.